

# OVERCOMING ELEMENT EROSION LIMITATIONS WITHIN LAGRANGIAN FINITE ELEMENT CODES

Rade Vignjevic<sup>(1)</sup>, Kevin Hughes<sup>(2)</sup>, Andrew Walker<sup>(3)</sup>, Emma A. Taylor<sup>(4)</sup>

<sup>(1)</sup> Structures and Materials Group, College of Aeronautics, Cranfield University, Cranfield, BEDS, MK43 0AL, UK, Rade.v@cranfield.ac.uk

<sup>(2)</sup> Structures and Materials Group, College of Aeronautics, Cranfield University, Cranfield, BEDS, MK43 0AL, UK, K.Hughes@cranfield.ac.uk

<sup>(3)</sup> Astrium Ltd, Gunnels Wood Road, Stevenage, SG1 2AS, UK, andrew.walker@astrium-space.com

<sup>(4)</sup> Astrium Ltd, Gunnels Wood Road, Stevenage, SG1 2AS, UK, Emma.taylor@astrium-space.com

## ABSTRACT

Lagrangian finite element methods have been used extensively in the past to study the non-linear transient behaviour of materials, ranging from crash test of cars to simulating bird strikes on planes.... However, as this type of space discretization does not allow for motion of the material through the mesh when modelling extremely large deformations, the mesh becomes highly distorted. This paper describes some limitations and applicability of this type of analysis for high velocity impacts. A method for dealing with this problem is by the erosion of elements is proposed where the main issue is the deformation of element failure strains. Results were compared with empirical perforation results and were found to be in good agreement. The results were then used to simulate high velocity impacts upon a multi-layered aluminium target, in order to predict a ballistic limit curve. LS-DYNA3D was used as the FE solver for all simulations. Meshes were generated with Truegrid.

## INTRODUCTION

Lagrangian finite element methods have been used extensively in the past to study the non-linear transient behaviour of structures. Due to their flexibility, the codes can also be applied to simulate high velocity impacts of orbital debris, in order to try and model as accurately as possible the resulting damage caused [1]. This enables the continuing development of different shielding configurations at a minimal expense – a factor that cannot be overlooked in today's competitive market.

As Lagrangian methods are based upon fixed mass elements, this means that when a structure deforms, so does the attached mesh. A direct consequence of this is that if a structure is subject to large deformations, then the mesh can become heavily distorted. These distorted elements can prove to be a real problem as they can cause the following undesirable effects; a reduction in time step leading to long run times, and a deterioration and break-up of the numerical integration process.

## OVERCOMING THE LIMITATION OF A LAGRANGIAN DISCRETIZATION

A numerical technique that deletes these heavily distorted elements, erosion algorithm, is usually

incorporated into Lagrangian codes and this allows the calculations to continue. This is accomplished by specifying an element failure strain, which if satisfied, results in the problem elements being deleted before they pose too much of a problem.

The element failure strain is a measure of the maximum allowed deformation of an element before it is deleted from the calculations. In LS DYNA3D, this value is determined by comparing the effective plastic strain to the plastic strain at failure for the material [2].

A direct consequence of using this erosion capability in the code is that as the elements are deleted, they no longer contribute to the physics of the simulated event. This means that the global system will lose both mass and energy, which can severely affect the evolution of a simulation. Therefore, to improve confidence to the results obtained from a simulation, the proper erosion characteristics have to be defined.

The determination of this value is not straightforward as if the failure strain is set too low, then the elements will be deleted too soon and the physics of the simulated event will not be represented.

For example, this is particularly important in simulations that involve the colliding of two objects. If the elements in the target material are deleted too soon, then the target material will lose mass, which will offer

even less resistance to the penetrating projectile, making it penetrate even further into the material than is realistic. Conversely, if the failure strain is set too high, the projectile may not perforate the target material and rebound, which is also unrealistic. The optimum response of the elements requires that the value lies between these two extremes.

One way of overcoming this limitation is by adjusting the value for the failure strain. The selection of values is essentially a trade off between prolonging an element's life for as long as possible, whilst at the same time, not sacrificing any computational time or accuracy as a result of the increasing deformation.

The paper by Murr et al. [3] discusses the application of the finite element method to the simulation of low to high velocity crater evolution of impact craters for different types of materials. One of the hurdles they encountered was this problem of selecting an appropriate value for the element failure strain for aluminium 1100. Conclusions from this paper were that values lying between 1 and 3 are acceptable, but for their simulations, a value of 1.5 was used to represent all materials. It bears no real relation to any physical effect. It is simply a way of relating the strain in an element to a threshold strain, which is a point at the onset of a degree of deformation where errors start to creep into both the time step and numerical integration. The effective plastic strain at failure can be used as a measure of failure, but also to stabilise and prolong a calculation.

The view behind this work is that further improvement in the simulation of low velocity impacts, can be made by using precisely defined failure criteria for the different materials present in the model.

#### CALIBRATION OF THE FAILURE CRITERIA

This paper deals with a method for calibrating values for the element failure strain for five different metals, namely Al6061-T6, Al5052, Al2024, Al2024-T4 and Stainless Steel T304.

As no experimental data was available, it was necessary to find a realistic erosion process, for which a simple simulation could be used to validate the selection of the values. Two different methods were adopted, enabling a direct comparison to be made between the two different approaches.

The first set of simulations involved using a crater prediction equation on a semi-infinite target. The other case considered was the complete perforation of a thin plate. A direct comparison between the two different

approaches would provide sufficient analytical proof that the methodology adopted was acceptable.

#### CRATER PREDICTION APPROACH

The idea behind these simulations was to scale the values for the failure strains of the elements until a predicted penetration depth was reached. The two parameters often associated with crater prediction are the penetration depth and the hole diameter, as shown in figure 1.

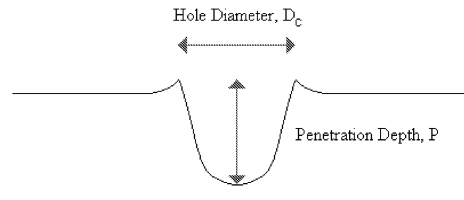


Figure 1 The two parameters used in empirical crater prediction models

The empirical equation developed by Cour-Palais and others, often takes the following form. It relates the penetration depth to the densities of the target and projectile and to the speed of the impact.

$$\frac{P}{d_p} = 2.28 \left( \frac{\rho_p}{\rho_t} \right)^{2/3} \left( \frac{u_0}{v_t} \right) \quad (1)$$

where  $P$  is the penetration depth,  $d_p$  is the projectile diameter,  $\rho_p$  and  $\rho_t$  are the projectile and target densities respectively,  $u_0$  is the impact velocity of the projectile and  $v_t$  is the speed of sound in the target material. (SI units were assumed throughout).

It was assumed that the velocity would be high enough that the hole diameter would be approximately the same as the diameter of the projectile, which was taken to be 5mm for this analysis. This same assumption was adopted by Baker [4]. Consideration was also not given to the amount of projectile remaining after the collision, as information on this aspect was not available.

Separate simulations were run which just consisted of an isotropic target material and projectile. The target material was cuboid in shape and had the dimensions (12x5x4.5)mm. With an element size of 0.25mm, the target material and projectile were meshed using 8 noded brick elements, with one point gaussian

quadrature. This resulted in 14,400 elements and 500 elements being created for the target and projectile components respectively. A Plastic kinematic material was assigned to both the projectile and the target. A symmetry plane was defined to reduce the number of elements in the model, and can be seen in figure 3.

Equation 1 was rearranged to solve for the velocity required in order to produce a crater which was arbitrarily chosen as being 3mm deep. As the projectile and the target were made out of the same material, the density terms drop out of the expression. The results for the variables can be found in table 1.

Material	Speed of Sound (ms <sup>-1</sup> )	Projectile Velocity (ms <sup>-1</sup> )
Al6061-T6	5055	682
Al5052	5110	690
Al2024 (-T6)	5103	689
S. Steel, T304	5000	675

Table 1 Predicted striking velocities in order to produce a 3mm deep crater for the different materials

The simulations were run for a variety of different failure strains and the penetration depth was recorded each time. The element failure strain was adjusted until the penetration depth of 3mm was reached. The resulting crater formed for Al6061-T6 can be found in figure 3, whereas the complete results for all the materials can be found in figure 4.

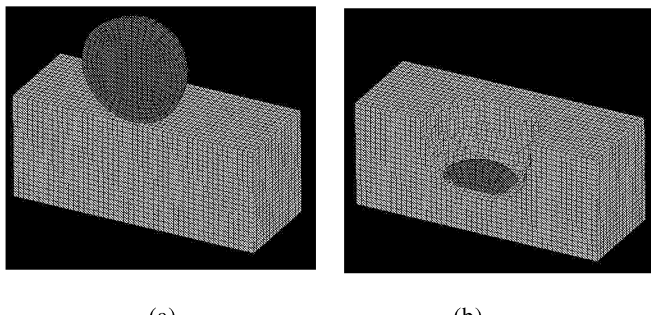


Figure 3 The resulting crater formed when the failure strain was set to 0.37μs for Al6061-T6 at 0μs (a) and 30μs (b)

The selection of the material failure strains for the different materials were simply read from the graph in figure 4. The conclusions from this part of the analysis is that the following element failure strains obtained via the crater prediction equations, should closely resemble a material's response subject to dynamic loading. A summary of the results can be found in table 2.

Material	Element Failure Criteria
Al6061-T6	0.39
Al5052	1.00
Al2024	1.25
S. Steel T304	0.56
Al2024-T4	0.35

Table 2 Element failure criteria for the different materials, obtained via the crater prediction approach

## VALIDATION

In order to add confidence to the values of the failure strains determined via the crater prediction approach, a comparison to experimental data was needed.

Results from empirical perforation equations were found in Zukas [5], which shows the ballistic limit curve for a variety of different thickness plates, subject to impacts from compact steel cylinders ( $L/d=1$ ).

According to the results [5], the ballistic limit of an aluminium plate constructed from Al2024-T4 with a  $T/d = 1.1$ , was determined to be in the region of  $400\text{ms}^{-1}$ . As the plate was 5.6mm thick, this meant that the projectile diameter was approximately 5mm.

As the projectile was compact, this meant that the height of the cylinder was also 5mm, so as to satisfy the condition that  $L/d = 1$ .

A separate simulation was now needed which consisted of a projectile constructed of stainless steel T304, with an element failure strain of 0.56, impacting a 5.6mm plate of Al2024-T4, which has an element failure strain determined to be 0.35. If perforation occurs at or around this velocity, then it is a small step to validating the usefulness of this approach.

The projectile was given a range of velocities in the range of 300 to  $400\text{ms}^{-1}$ . Using the values for the failure strains defined in table 2, the penetration depth was recorded each time. The results can be seen in figure 5. The results show that the projectile just manages to perforate the target plate at  $400\text{ms}^{-1}$ . This means that on the basis of this initial testing of the erosion process, the results for predicting the element failure strains for the different materials appears to hold. However further testing is needed in order to more accurately validate this approach.

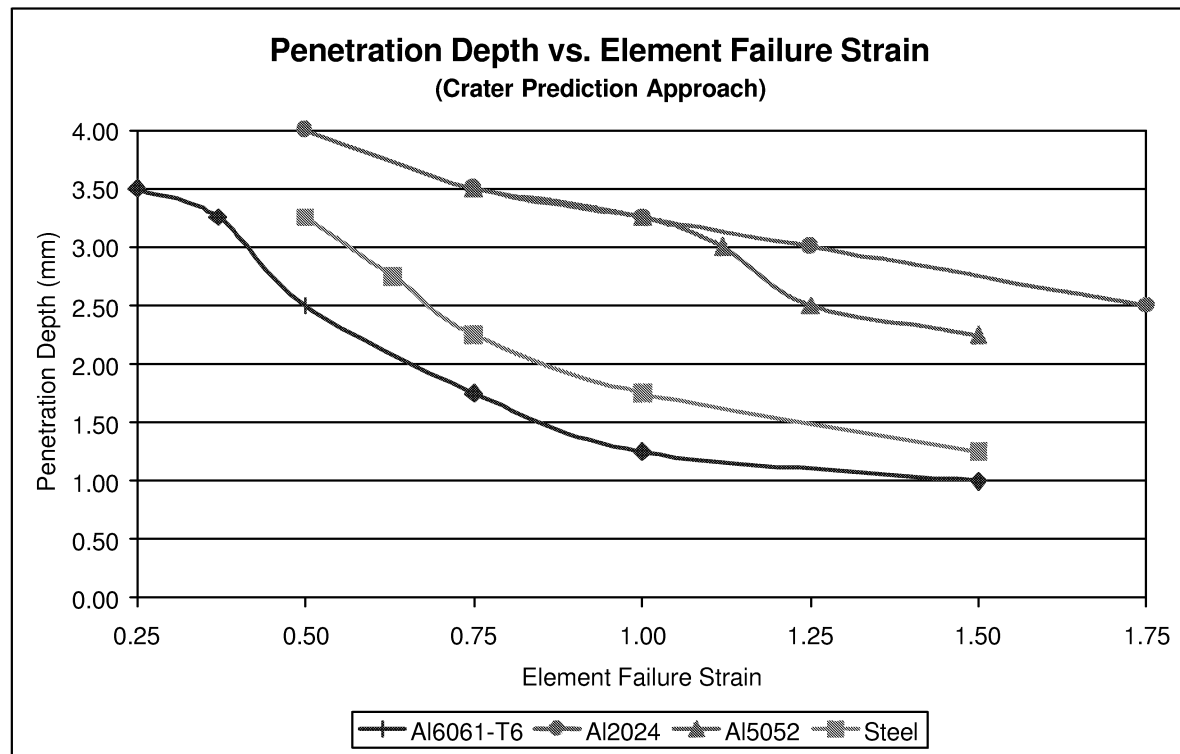


Figure 4 Penetration depth vs. Element failure strain for four different materials, which were obtained via the cratering prediction approach

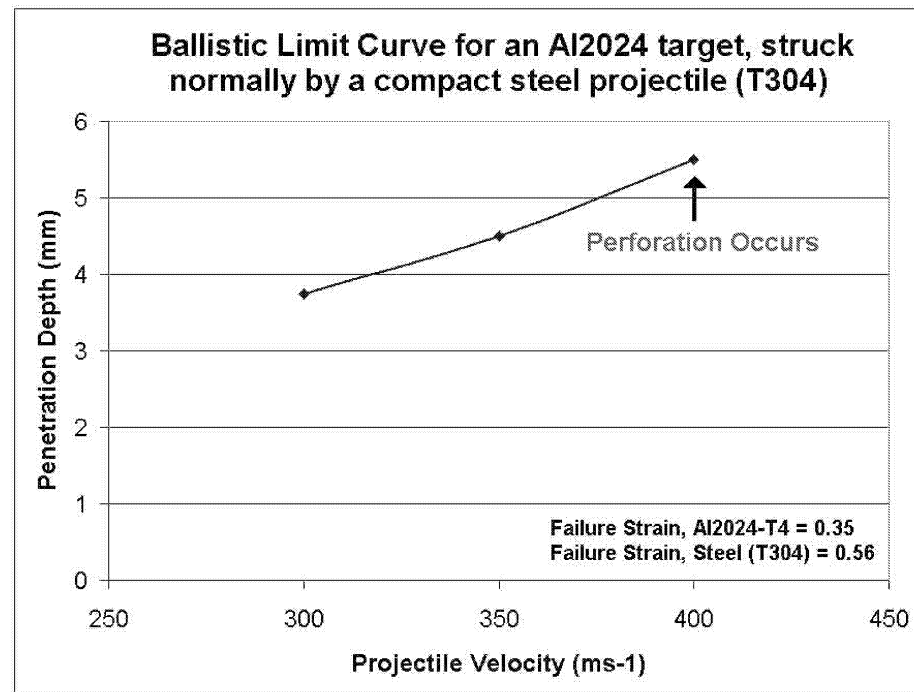


Figure 5 Results of the validation simulations to determine the accuracy of the element failure strains. They are found to be in good agreement with empirical perforation data.

## APPLICATION

The overall aim of this work is to try and accurately predict a ballistic limit curve for a multi-material target. A ballistic limit curve can be used to assess the impact resistance of a structure, by providing the critical velocity at which perforation or failure of the target material occurs.

The idea behind choosing this idea of a ballistic limit curve is that this scenario is very material specific. If the wrong material properties are used, then this will have a massive effect on the resulting behaviour of the target material. Another constraint based upon the resulting behaviour is the selection of values for the element failure strain.

It is hoped that with no experimental data available, the crater prediction approach is a valid way of determining the material specific element failure strains.

## TARGET MATERIAL

The target material consists of an aluminium housing (Al6061-T6) sandwiched between two aluminium facesheets (Al2024). The housing is used to protect an internal component. The entire model contained approximately 17 thousand elements and can be seen in figure 6.

The aim was to investigate the damage caused by a wide range of projectile sizes and velocities, initially striking normally, along the symmetrical axis of the housing. The selection of this type of design was chosen so as to demonstrate the capabilities of the erosion algorithm and how a realistic representation of the values completely dominates the resulting material behaviour.

The purpose of which was to enable ballistic limit curves to be defined, which showed the range of values at which significant damage is experienced by the internal component.

The criteria for failure were taken to be either complete perforation, or a reduction in the cross-sectional area, which was arbitrarily chosen as being 20%.

Initially, simulations were run for the 5mm-diameter projectile. As the run time for the simulations varied between 6 and 18 hours, (depending upon the velocity of the projectile), it was necessary to find a quick method of converging to the critical velocity. This was accomplished by making an initial guess. If this value was not suitable, then the velocity was halved each

time, and either added to or subtracted from the previous guess. This was deemed to be the fastest way of obtaining the right answer.

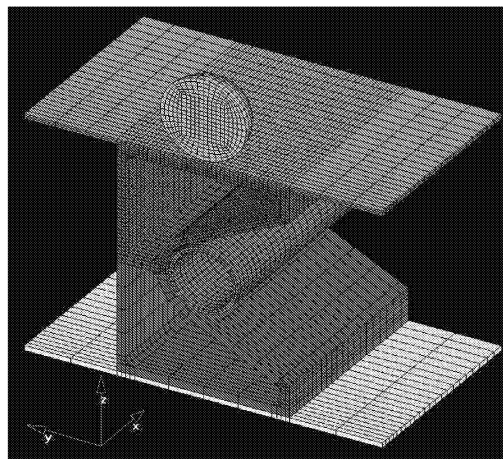


Figure 6 Isometric view of the target and projectile, showing the symmetry plane created

A typical set of results can be seen in the diagrams in figure 7. It shows the resulting deformation caused by a 5mm-diameter projectile impacting at  $500\text{ms}^{-1}$ . The initial configuration can be seen in figure 7-a. As the target material starts to deform, (figures 7-b), it is possible to see the element erosion that is taking place.

After  $24\mu\text{s}$  (figure 7-c), the projectile is starting to press down on the upper arm of the housing, which in turn is starting to bite down on the component it is trying to protect.

The final snapshot shown in figure 7-d, shows the resulting deformation of the internal component. After  $50\mu\text{s}$ , the projectile, which is still intact, is brought to rest. The  $500\text{ms}^{-1}$  impact has resulted in a 20% reduction in the cross-sectional area, and is therefore the critical velocity for this size of projectile.

The simulations were then repeated for a variety of different projectile sizes, but due to the long run times and the iterations required in order to home in on the correct velocity, not many results were collected. In fact, it was only possible to collect data for three different projectile diameters, the results of which can be found in table 3.

Projectile Diameter(mm)	Ballistic Limit Velocity ( $\text{ms}^{-1}$ )
3	1100
4	750
5	500

Table 3 Ballistic limit velocities for the multi-material target

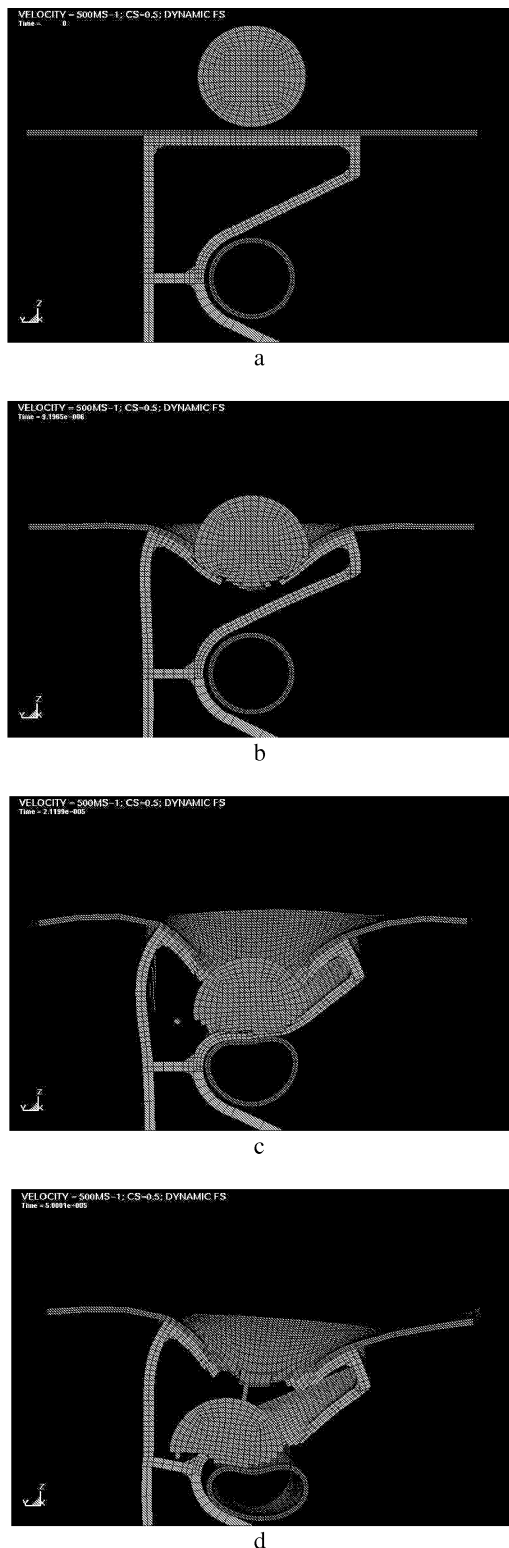


Figure 7 The resulting deformation caused by a 5mm projectile impacting at  $500\text{ms}^{-1}$  at (a) 0µs, (b) 12µs, (c) 24µs and (d) 50µs

## CONCLUSIONS

The purpose of this paper was to describe a method of obtaining representative values for the element failure strain for different materials. The ultimate aim was to add credence to the values chosen, so that there can be an increase in confidence to the results obtained in situations where an accurate representation of a materials response is critical.

The values were obtained using an empirical cratering equation, which were then cross-checked with empirical perforation data. The results were in close agreement, but this work could be extended to consider the amount of projectile that is left intact after the impact, as well as to the residual velocity of the projectile.

These two further improvements would further refine the values for the element failure strains, enabling a more realistic representation of a material's response.

The results were then used to predict the resulting deformation of high velocity impacts on a multi-material aluminium target. As was demonstrated, the values of the failure strains (i.e. which controlled when a distorted element becomes deleted) is critical to the predicted behaviour.

This work was made as accurate as is humanly possible with only analytical data, it still remains to be seen as to whether or not the values are in close agreement with actual experimental data, whether this be via cratering experiments, or actual impacts on targets. From the initial work reported in this paper, this method appears to be a valid approach in overcoming the limitations in Lagrangian finite element codes.

## ACKNOWLEDGEMENTS

The work presented in this paper was submitted in partial fulfilment of the requirements for the degree of Master of Science (Cranfield University, UK), and could not have been accomplished without the help provided Dr. Rade Vignjevic and Tom De Vuyst, who are both from Cranfield University.

## REFERENCES

- [1] Campbell, J. Lagrangian hydrocode modelling of hypervelocity impact on a spacecraft, PhD. Thesis, Cranfield University, 1998

- [2] LSTC. LS-DYNA : Keyword User's Manual : Non-linear dynamic analysis of structures, LSTC, Version 950, May 1999
- [3] Murr, L.E., et al. *The low velocity to hypervelocity penetration transition for impact craters in metal targets*, Material Science and Engineering A, Volume 256, Issue 1-2 : 166-182, November, 1998
- [4] Baker, J.R, Hypervelocity crater penetration depth and diameter – a linear function of *impact velocity?*, International Journal of Impact Engineering, Volume 17, 25-35, 1995
- [5] Zukas, J.A. High Velocity Impact Dynamics, John Wiley & Sons, 1990, p460